Energy &
Environmental
Science

REVIEW

View Article Online
View Journal | View Issue

Cite this: *Energy Environ. Sci.*, 2020, **13**, 3253

Seawater electrolyte-based metal–air batteries: from strategies to applications

Jia Yu, Bo-Quan Li, Chang-Xin Zhao and Qiang Zhang*

Received 20th May 2020,
Accepted 11th August 2020

DOI: 10.1039/d0ee01617a

rsc.li/ees

Aqueous metal–air batteries are promising next-generation energy storage and supply technologies due to their advantages of high energy density and intrinsic safety. As an abundant natural resource, applying seawater-based electrolytes is proposed to have considerable economic and environmental benefits, and will significantly broaden the applications of metal–air batteries. However, the existence of complex components in seawater, in particular chloride ions, inevitably has a complex influence on air electrode processes, including the oxygen reduction and evolution reactions (ORR and OER), requiring the development of efficient chloride-resistant electrocatalysts. Meanwhile, a few seawater-based metal–air battery prototypes have shown great application potential but are still at an early stage of development. In this review, we first propose the concept of seawater-based metal–air batteries and comprehensively analyze the essential air electrode reactions in terms of thermodynamics and kinetics. Subsequently, rational design strategies for ORR and OER electrocatalysts suitable for use in chloride-containing and seawater-based electrolytes are comprehensively discussed. Moreover, the development history and potential applications of seawater-based metal–air batteries are demonstrated. Finally, a summary and outlook are provided for future innovations.

Broader context

With higher theoretical energy densities and intrinsic safety, aqueous rechargeable metal–air battery technology is considered to be a promising alternative to widely-used lithium ion batteries. As an extremely abundant (~96.5% of the amount of total water on Earth) and almost zero-cost resource, the possible application of seawater in metal–air battery electrolytes will greatly reduce battery costs, broaden application areas, and enhance environmental friendliness. However, the complex seawater components inevitably hinder the air electrode reactions that are critical for battery performance. In particular, the existence of chloride ions can inhibit the ORR/OER kinetics *via* multiple mechanisms. Therefore, the development of seawater-based metal–air batteries relies on highly active, selective, and stable ORR/OER electrocatalysts suitable for a seawater environment, where an in-depth understanding of the relevant influencing mechanisms is a prerequisite and some key progress has been achieved in recent years. In this review, current understanding of the ORR/OER electrocatalytic mechanisms in the presence of chloride ions as well as key progress relating to electrocatalyst design strategies for chloride-containing and seawater-based electrolytes are highlighted. It aims to provide guidance for enhancing ORR/OER processes in seawater-based metal–air batteries, and the relevant electrocatalyst strategies and methodologies based on complex seawater systems could inspire other electrochemical energy technologies, contributing to clean energy systems in a future fossil-fuel-free society.

1. Introduction

Recently, the continuing consumption of fossil fuels has resulted in a serious energy crisis as well as environmental problems, which are propelling the utilization of renewable energy sources (*e.g.*, solar, wave, wind, and geothermal).[1–3] Since they are usually abundant but intermittent, this drives us to employ efficient storage and conversion technologies to transform them into electrochemical energy. As one of the most widely used electrochemical energy technologies nowadays, lithium ion batteries (LIBs) face multiple problems, including the tight supply of cobalt and safety risks originating from organic electrolytes. Meanwhile, their energy density is seriously restricted by the capacity of the electrode material.[4] These factors have promoted worldwide research into alternative rechargeable batteries. Aqueous rechargeable metal–air batteries (*e.g.*, zinc–air, magnesium–air, and aluminum–air batteries) generate electricity *via* the redox reactions between active metal anodes and oxygen at the cathodes. They are considered promising alternatives to LIBs owing to the low cost originating from the active materials, intrinsic safety originating from aqueous electrolytes, and high theoretical energy density originating from the infinite supply of oxygen.[5]

Over the decades, quite a few metal–air battery systems have been developed, mainly operating with conventional aqueous

Beijing Key Laboratory of Green Chemical Reaction Engineering and Technology, Department of Chemical Engineering, Tsinghua University, Beijing 100084, China. E-mail: zhang-qiang@mails.tsinghua.edu.cn

electrolytes consisting of high-purity distilled water in which alkalis, acids, or buffers are solvated.[6] As is well known, seawater is sufficiently available on Earth (∼96.5% of the total amount of water) with a relatively homogeneous geographical distribution. Therefore, the possible replacement of distilled water with seawater in the electrolyte offers great advantages: (1) reducing the costs of electrolytes and metal–air battery systems; (2) alleviating competition with the consumption of fresh water by human activities; (3) broadening application areas where seawater is sufficiently available, such as islands and the ocean.[7] Currently, although the majority of seawater usage in energy fields focuses on electrochemical and photoelectrochemical water splitting devices,[8–10] several metal–air battery prototypes using seawater electrolytes and submerged reactive metal anodes have been reported.[11,12] However, the exploitation of seawater in the metal–air battery field is still at an early stage.[13]

When compared with conventional electrolytes based on distilled water, applications of seawater-based electrolytes in metal–air batteries are quite promising yet challenging because of the complex components of seawater. As the main constituent, the existence of chloride ions inevitably hinders the air electrode reaction processes. Briefly, the energy efficiency of a rechargeable metal–air battery is predominantly determined by its air electrode part, where the oxygen reduction and evolution reactions (ORR and OER) occur during discharging and charging, respectively, as the core processes of the battery.[14,15] To enhance the inherently sluggish ORR/OER kinetics, which cause the major energy efficiency loss in batteries, a series of highly active electrocatalysts have been developed and integrated into the air electrode, such as noble-metal-based materials (*e.g.*, Pt, Ir, and relevant derived compounds) as well as their inexpensive alternatives (*e.g.*, carbon-based nanomaterials, transition metal oxides/chalcogenides/hydroxides),[16–19] with various

Jia Yu

Jia Yu received his BS degree from the University of Science and Technology of China and his PhD degree from the Institute of Process Engineering, Chinese Academy of Sciences. In 2018, he joined Prof. Qiang Zhang's group as a postdoctoral researcher at the Department of Chemical Engineering of Tsinghua University. His current research interests focus on optimization strategies relating to ORR/OER bifunctional electrocatalysts for Zn–air batteries and electrocatalytic reaction kinetics under extreme environments.

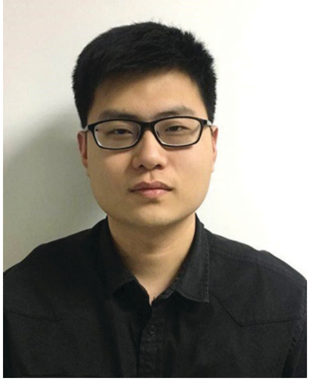

Bo-Quan Li

Bo-Quan Li received his BS degree from the Department of Chemistry, Tsinghua University and his PhD degree from the Department of Chemical Engineering, Tsinghua University. He is currently an assistant professor in the Advanced Research Institute of Multidisciplinary Science, Beijing Institute of Technology. His current research interests are energy storage chemistry and materials for lithium–sulfur batteries, lithium metal batteries, metal–air batteries, and oxygen electrocatalysis.

Chang-Xin Zhao

Chang-Xin Zhao obtained his BS degree at Tsinghua University in 2019. He is currently a PhD student at the Department of Chemical Engineering, Tsinghua University. His research interests focus on advanced energy materials for lithium–sulfur batteries and oxygen electrocatalysis.

Qiang Zhang

Qiang Zhang is a full professor at Tsinghua University. He held the Newton Advanced Fellowship from the Royal Society, UK, and the National Science Fund for Distinguished Young Scholars. He was selected as a highly cited researcher in 2017, 2018, and 2019 by Clarivate Analytics. His current research interests are advanced energy materials, including dendrite-free lithium metal anodes, lithium sulfur batteries, and electrocatalysis, especially the structural design and full demonstration of advanced energy materials in working devices. He is an associate editor of J Energy Chem and Energy Storage Mater. He also sits on the Editorial Boards of Matter, Adv Funct Mater, J Mater Chem A, Chem Commun, and others.

electronic and structural regulation.[20–24] These electrocatalysts usually exhibit superior activity in conventional electrolytes; nevertheless, the chloride environment will inevitably result in undesirable side effects during the air electrode process, not to mention direct operation with seawater-based electrolytes with more complex components. For example, the chloride ion adsorption behavior blocks the active sites during ORR,[25] the chlorine oxidation reactions compete with OER,[26,27] and accelerated corrosion or degradation of the electrocatalysts occurs. In particular, the chloride adsorption inhibition and competitive inhibition factors greatly hinder the cathodic and anodic electrocatalytic reactions, respectively.

Therefore, understanding the electrocatalytic mechanisms in seawater systems is of great importance for developing active, stable, and selective electrocatalysts for metal–air batteries using seawater-based electrolytes (or seawater-based metal–air batteries). It is worth noting that the electrocatalytic performance depends not only on the intrinsic activity of the electrocatalysts, but also on their multiscale architectural design, which determines the exposure of active sites and mass/electron transfer.[28] Based on a systematic study of the influences of chloride ions on the ORR/OER processes, we comprehensively summarize the componential and architectural design strategies for efficient chloride-resistant ORR/OER electrocatalysts. And then electrocatalyst strategies for direct operation with seawater-based electrolytes are discussed in detail. Furthermore, potential applications and design principles of seawater-based metal–air batteries are analyzed, accompanied by several successful prototypes.

2. Concept and mechanisms

2.1. Concept of seawater-based metal–air batteries

In general, seawater-based metal–air batteries share similar cell structures with conventional metal–air batteries, except for the use of seawater-based electrolytes. Typically, a rechargeable seawater-based metal–air battery should be mainly composed of an air cathode comprising oxygen electrocatalysts and a gas diffusion layer, a reactive metal anode, and, more importantly, a seawater-based electrolyte (Fig. 1). In some cases when using highly active anodes, such as Na metal, the anode and cathode compartments are supposed to be separated by a selective cation-conducting membrane.[13,29] During discharging, it supplies energy *via* electrochemically coupling the metal anode to the air cathode in the presence of seawater components.[2] Electrons are liberated from the metal anode and travel to the air cathode *via* an external channel, while metal hydroxides, metal acid anions, or metal cations are produced in terms of the electrolyte environment. Meanwhile, ambient oxygen is diffused into the air cathode and then reduced to hydroxide ions or water molecules *via* the ORR process, at a three-phase reactive interface between oxygen, the electrolyte, and the electrocatalysts. During charging, the battery stores electrical energy *via* OER at the air electrode, whereas metal is deposited at the anode. Considering the partial pressure of O_2 ($P_o \approx 0.206$ atm), the ORR/OER electrocatalytic reactions in the air electrode at room temperature are stated below (eqn (1) and (2)), where the potentials are referenced to a standard hydrogen electrode (SHE).[30]

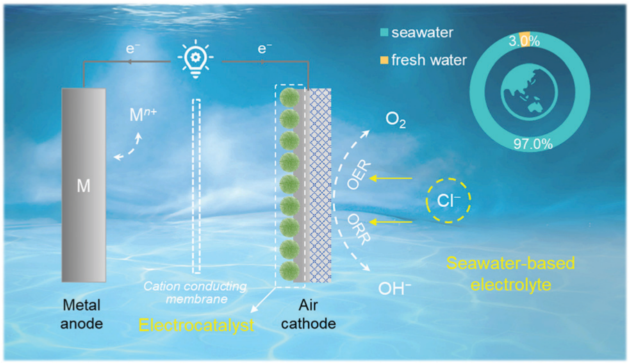

Fig. 1 A schematic illustration of the basic structure and operating mechanism of a rechargeable metal–air battery using a seawater-based electrolyte, accompanied by the relevant application values.

$$O_2 + 2H_2O + 4e^- \leftrightarrow 4OH^- \text{ (alkaline conditions)} \quad (1)$$

$$O_2 + 4H^+ + 4e^- \leftrightarrow 2H_2O \text{ (acid conditions)} \quad (2)$$

$$\phi = 1.22 \text{ V} - 0.059 \text{ pH } vs. \text{ SHE}$$

Seawater is a multi-component solution with a medium salinity of ~3.5% and a high ionic conductivity of ~50 mS cm^{-1}, showing considerable potential to replace distilled water in aqueous electrolytes. However, seawater has various additional dissolved ions (*e.g.*, Cl^-, Na^+, SO_4^{2-}, Mg^{2+}, Ca^{2+}, *etc.*), where Cl^- (~0.54 M) plays the main role (Fig. 2a). Therefore, the applications of seawater-based

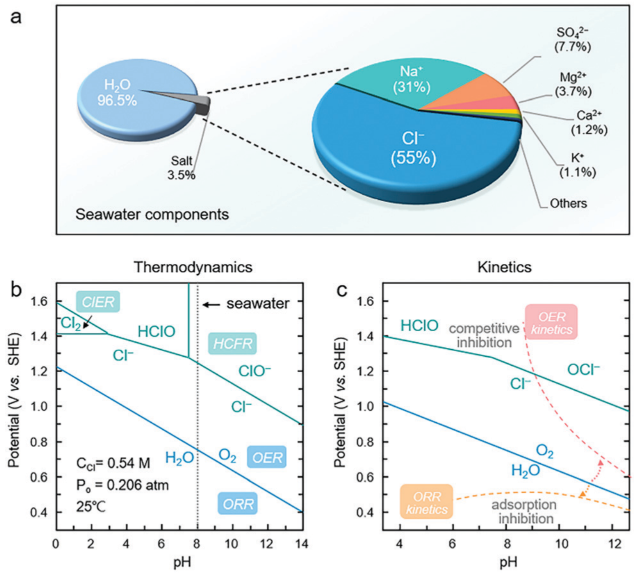

Fig. 2 The scientific feasibility of seawater-based metal–air batteries. (a) A pie diagram of the components in seawater. (b) A simulated Pourbaix diagram of seawater in terms of thermodynamics at 25 °C, with a total chlorine concentration of 0.54 M, an O_2 partial pressure of 0.206 atm, and activity coefficients of 1 for all species. (c) A simulated Pourbaix diagram of seawater in terms of kinetics, considering the chloride adsorption behavior during the ORR and competitive chloride oxidation reactions during the OER.

electrolytes inevitably face great challenges originating from the interference effects of chloride ions on electrocatalytic reactions.

2.2. Thermodynamics of the ORR/OER in seawater

From the perspective of thermodynamics, theoretically there exist a complex ensemble of possible oxygen/chlorine redox reactions in the electrochemical processes in seawater, which depend on pH, the oxygen/chlorine concentration and temperature. Obviously, O_2 provided from the surrounding atmosphere or seawater participates in the ORR/OER processes during discharging/charging. In contrast, Cl^- in seawater may participate in the hypochlorite formation reaction (HCFR) or chlorine evolution reaction (ClER) to generate hypochlorite or chlorine byproducts during charging, while the chlorine reduction reaction will not occur in the absence of Cl_2 during discharging. Considering the total chlorine concentration of 0.54 M in seawater, the chlorine electrocatalytic reactions at room temperature are given below (eqn (3)–(5)):

$$Cl^- + 2OH^- - 2e^- \rightarrow ClO^- + H_2O \text{ (alkaline conditions)} \tag{3}$$

$$\phi = 1.71\ \text{V} - 0.059\ \text{pH } vs.\ \text{SHE}$$

$$Cl^- + H_2O - 2e^- \rightarrow HClO + H^+ \text{ (acid conditions)} \tag{4}$$

$$\phi = 1.49\ \text{V} - 0.030\ \text{pH } vs.\ \text{SHE}$$

$$Cl^- - 2e^- \rightarrow Cl_2 \text{ (acid conditions)} \tag{5}$$

$$\phi = 1.41\ \text{V } vs.\ \text{SHE}$$

Fig. 2b illustrates the simulated Pourbaix diagram of oxygen/chlorine electrochemistry in seawater. During the discharge process of seawater-based metal–air batteries, O_2 is easily reduced through the ORR process whose electrode potential is far higher than that of the metal oxidization reaction (not shown in the diagram). During the charge process, OER is thermodynamically favored over HCFR and ClER whether in alkaline or acid conditions, with various electrode potential differences. Concretely, the OER electrocatalysts operating at an overpotential $<$490 mV in alkaline conditions can theoretically prevent the HCFR process in a seawater-based electrolyte, although it is challenging at relatively high current densities. Below the pK_a of HClO (7.4), HClO formation becomes dominant instead of ClO^-, and the oxygen/chlorine potential difference becomes slightly smaller. Furthermore, ClER becomes the dominant chlorine oxidation reaction at pH $<$ 2.9, whose equilibrium potential is close to but still 100–200 mV higher than that of OER. Therefore, seawater-based metal–air batteries render thermodynamic feasibility in the presence of Cl^-, while alkaline conditions are preferable for the OER process.[27]

2.3. Kinetics of the ORR/OER in seawater

As discussed above, both ORR and OER are thermodynamically favorable during the electrochemical processes in seawater, but the kinetic factors which determine the practical performance of seawater-based metal–air batteries are more complicated. In fact, exposing electrocatalysts to chloride ions will give rise to a serious inhibition effect in reaction kinetics.

Primarily, ORR electrocatalysts usually suffer from a specific Cl^- blocking effect due to its strong adsorption on the active sites compared with other anions such as ClO_4^- (weak adsorption) or HSO_4^- (modest adsorption).[31] In this case, a large fraction of the active sites cannot be directly exposed to the reactants while the adsorption energy of neighboring adsorption sites is also changed; thus the adsorption of O_2 molecules is suppressed. These blocked sites make little contribution due to poor accessibility and greatly hinder the electrocatalyst activity to render an overpotential as high as several hundred millivolts (Fig. 2c).[25,32] Meanwhile, the reversibility of Cl^- adsorption is still controversial.[33] Besides the blocking effect, Cl^- adsorption also affects the breaking of O–O bonds to induce a two-electron transfer ORR pathway with solution phase H_2O_2 formation, rather than a four-electron pathway.[31] Considering the partial pressure of O_2 ($P_o \approx 0.206$ atm), the two-electron ORR reactions at room temperature are stated below (eqn (6) and (7)).[30]

$$O_2 + H_2O + 2e^- \rightarrow HO_2^- + OH^- \text{ (alkaline conditions)} \tag{6}$$

$$\phi = 0.35\ \text{V} - 0.030\ \text{pH } vs.\ \text{SHE}$$

$$O_2 + 2H^+ + 2e^- \rightarrow H_2O_2 \text{ (acid conditions)} \tag{7}$$

$$\phi = 0.68\ \text{V} - 0.059\ \text{pH } vs.\ \text{SHE}$$

The presence of H_2O_2 at the multiphase interface will generate free radicals and attack the electrocatalysts and metal anodes, consequently causing degradation in durability.[34,35] Both the Cl^- blocking and H_2O_2 formation effect are highly related not only to the electrocatalyst chemical structure which determines the intrinsic activity, but also to the electrocatalyst architectural structure from the microscale exposed crystal surface to the macroscale three-dimensional structure. In addition, metal dissolution and surface passivation caused by the formation of soluble chloride complexes (*e.g.*, $PtCl_4^{2-}$) also lead to detrimental effects on ORR stability to some extent.[36,37]

On the other hand, although OER is thermodynamically favored over HCFR/ClER during the charge process of seawater-based metal–air batteries, HCFR/ClER will compete with OER in terms of reaction kinetics, because HCFR/ClER are two-electron oxidation reactions that involve only one single intermediate, while OER is based on a complex four-electron pathway which needs to remove four protons and involves three intermediates.[38–40] More importantly, OER electrocatalysts are usually proficient in the catalytic oxidation of chloride ions, since the two reactions partially share similar active sites and pathways.[41,42] Rossmeisl *et al.* found a scaling relation between the binding energetics of ClER and OER intermediates by calculations on presumed mechanisms, indicating that electrocatalysts that tend to bind oxygen-bound intermediates will bind chloride-bound intermediates too.[43] Similarly, Over *et al.* found that OER and ClER occurring on the $RuO_2(110)$ surface share the same active sites based on simulation results: oxygen atoms bound to Ru atoms which are unsaturated on the surface.[44,45]

As shown in Fig. 2c, the sluggish OER kinetics leads to a considerable overpotential which induces competitive inhibition of HCFR/ClER on OER in seawater, as detrimental side reactions.

This competition is highly dependent on pH, current density, and Cl^- concentration.[46] The standard electrode potential of OER is relatively far below the HCFR potential in a strong alkaline environment, but considering the kinetics, the actual difference will obviously decrease or even reverse with a decreasing pH value. Alkaline conditions are therefore more suitable for selective OER in seawater from the kinetics aspect, that HCFR cannot occur if the electrocatalyst enables a low enough overpotential. By contrast, acid conditions are highly challenging when OER and ClER are thermodynamically close in equilibrium potential to make the kinetic issue more decisive. Like the Cl^- adsorption inhibition during ORR, the Cl^- oxidation competitive inhibition during OER can be regulated by multiple compositional and architectural factors of the electrocatalysts. In fact, ClER is the dominant anodic reaction in acid conditions for quite a number of oxide electrocatalysts.[41,43,47] Currently chlorine and hypochlorite are valuable products in the chlor-alkali and wastewater treatment industry, when relevant research on oxygen–chlorine competition focuses mainly on selectivity toward ClER rather than OER.[41,48,49] In addition, when compared with the ORR process, aggressive Cl^- and possible chlorine/hypochlorite byproducts corrode the OER electrocatalysts and metal anodes more heavily through formation of metal chloride–hydroxide.[50]

Therefore, despite their thermodynamic feasibility, two key kinetic issues concerning air electrode processes in seawater-based metal–air batteries are Cl^- adsorption inhibition during ORR and Cl^- oxidation competitive inhibition during OER. For the former, the critical point is to inhibit Cl^- blocking and two-electron reduction reactions in ORR by using selective adsorption-resistant and four-electron pathway electrocatalysts. For the latter, the critical point is to inhibit the competition of the chlorine oxidation reaction against OER, where the acid/alkaline conditions play a determinable role in OER selectivity. Based on these considerations, we can generalize the design criteria for chloride-resistant ORR/OER electrocatalysts with desired activity, selectivity, and stability, which can be regulated by multiple aspects, including intrinsic electrocatalytic performance, multiscale structure design, and surface/interface engineering.[26,51–54]

3. Electrocatalysis in seawater-based electrolytes

The practical working discharge/charge voltages of a rechargeable metal–air battery are lower/higher than corresponding standard voltages in consideration of the internal loss, including the activation, ohmic polarization and concentration loss.[55,56] The sluggish ORR/OER kinetics give rise to large overpotentials and thus the redox reactions in the air electrode become a performance bottleneck in metal–air batteries.[57] Generally, in order to achieve efficient ORR/OER processes, the electrocatalysts should possess the following characteristics: (I) high intrinsic activity for reduced activation energies, (II) high density and homogeneous distribution of active sites for promoted accessibility to reactants, (III) a large surface area with abundant porosity for facile mass transfer, (IV) good mechanical and chemical stability for long-term durability, and (V) favorable conductivity properties for accelerated electron conduction.[16] However, to achieve efficient electrocatalytic processes in seawater-based metal–air batteries, it is necessary to endow the electrocatalysts with specific resistance to the complex seawater environment. Relevant electrocatalyst strategies will be discussed in detail, from various aspects of chloride-containing electrolyte and seawater-based electrolyte.

3.1. Chloride-resistant ORR electrocatalysts

The electrocatalytic processes in chloride-containing electrolytes lay the foundation for applications of seawater-based electrolytes in metal–air batteries. The main challenge for ORR in chloride-containing electrolytes is Cl^- adsorption on the active sites, which seriously hinders the electrocatalytic performance even using originally terrific ORR electrocatalysts. Research on this problem revealed that both aspects of intrinsic activity and structural regulation are worthy of attention.

First, the ORR performance of electrocatalysts in a chloride-containing environment relies heavily on their intrinsic resistant ability. In general, noble-metal-based electrocatalysts are highly susceptible to Cl^- poisoning, such as Pt-based materials.[31]

However, Ziegelbauer *et al.* reported that Rh-based electrocatalysts such as Rh_xS_y could exhibit considerable stability in a chloride environment to some extent.[60,61] Moreover, compared with the majority of noble-metal-based materials, noble-metal-free and especially metal-free electrocatalysts are more resistant to Cl^- and consequently are regarded as promising alternatives. Ozkan *et al.* systemically investigated the chloride-poisoning resistance of various ORR electrocatalysts, revealing that nitrogen-doped carbon (CN_x) and Fe,N co-doped carbon (FeNC) well maintain their ORR activities upon exposure to chloride compared with Pt/C or Rh_xS_y/C (Fig. 3a).[58] Concretely, with the addition of 100 mM Cl^- to a 0.5 M H_2SO_4 electrolyte, the ORR half-wave potential ($E_{1/2}$) of Pt/C, Rh_xS_y, and FeNC decreased by 490 mV (0.81 to 0.32 V), 140 mV (0.68 to 0.54 V), and only 50 mV (0.69 to 0.64 V), respectively. And CN_x demonstrated the highest resistance to Cl^- poisoning with an unexpected 30 mV increase in $E_{1/2}$, despite its relatively low original ORR activity ($E_{1/2}$ of 0.55 V). It is suggested that chlorine atoms incorporated into the carbon matrix result in a positive charge on the adjacent carbon atoms and facilitate the adsorption of O_2 on these sites, because of the higher electronegativity of Cl (3.16) over C (2.55) (Fig. 3b). Other possible mechanisms are associated with an increased density of active sites, or a synergistic effect between N and incorporated Cl.[58] Analogously, when exposed to other poisoning contents, including CO, H_2S, and CN^-, the ORR electrocatalysts without metal-centered active sites demonstrate high resistance, rendering the great potential of metal-free electrocatalysts in complex electrolyte environments.[62,63]

In addition to developing noble-metal-free materials with intrinsic chloride-poisoning resistance, optimizing the existing noble-metal-based ORR electrocatalysts is attractive due to their state-of-the-art activity, where structural design is a promising strategy. Based on atomic-scale structural sensitivity, exposing a highly selective facet as much as possible can efficiently

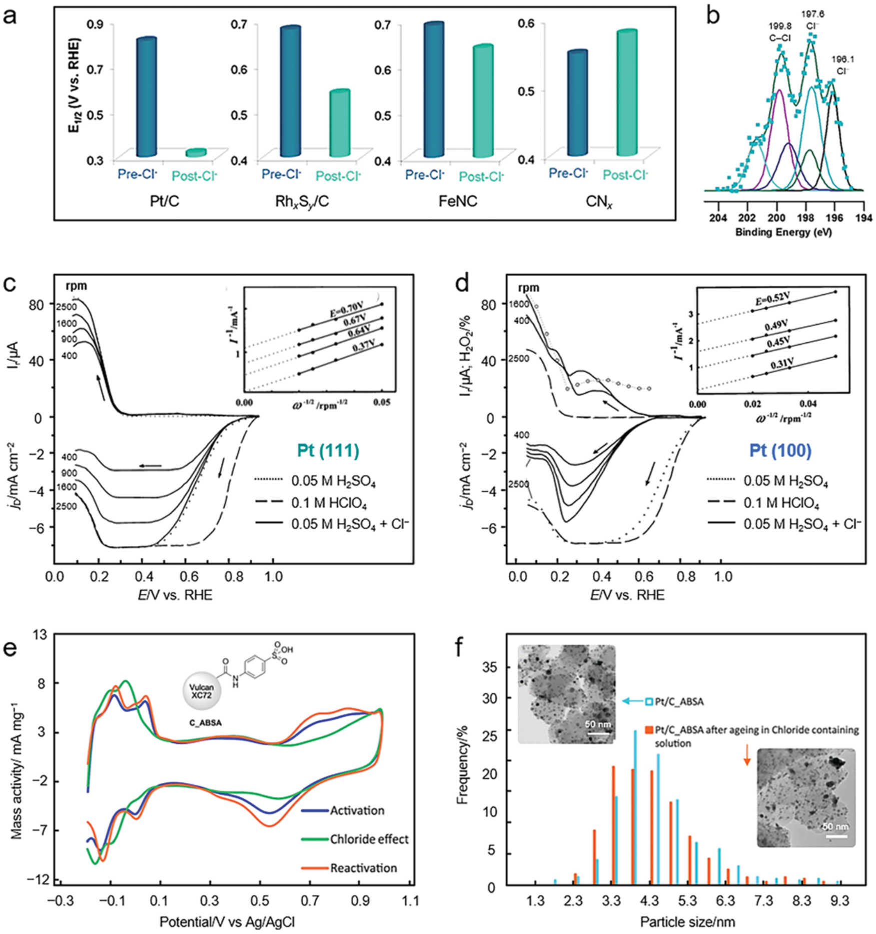

Fig. 3 Chloride-resistant ORR electrocatalysts. (a) A comparison of the ORR $E_{1/2}$ values of Pt/C, Rh_xS_y/C, FeNC, and CN_x electrocatalysts before and after adding 100 mM NaCl to 0.5 M H_2SO_4 electrolyte.[58] (b) The Cl 2p XPS spectrum of CN_x soaked in 0.5 M HCl.[58] Copyright 2017, Springer Nature. (c and d) The ORR polarization curves of Pt(111) and (100) on disk electrodes in 0.1 M $HClO_4$, 0.05 M H_2SO_4, and 0.05 M H_2SO_4 + 1 mM Cl^-, and the corresponding peroxide oxidation currents on ring electrodes (insets: Levich plots at various potentials).[25] Copyright 2001, Elsevier. (e) CV curves of a Pt/C_ABSA electrocatalyst in 0.5 M H_2SO_4 (activation), 0.5 M H_2SO_4 + 5 mM NaCl (chloride effect), and 0.5 M H_2SO_4 (reactivation), successively (inset: the molecular diagram of C_ABSA).[59] (f) The size distributions of Pt particles in Pt/C_ABSA before and after cycling in 0.05 M H_2SO_4 + 25 mM Cl^- (insets: corresponding transmission electron microscopy (TEM) images).[59] Copyright 2016, Elsevier.

inhibit the Cl^- blocking effect and maintain the original activity. For example, Markovic and co-workers studied the ORR kinetics of Pt(111) and (100) crystal facets influenced by structure-sensitive adsorption of Cl^-.[25] The ORR kinetics on the Pt(111) surface in a 0.05 M H_2SO_4 electrolyte were only negligibly reduced after introducing 1 mM Cl^- (Fig. 3c). And the Levich–Koutecky plots delivered a B value of $\sim 4.2 \times 10^{-2}$ mA $rpm^{-0.5}$, which indicated a 4 e^- reduction pathway.[64–66] In contrast, the ORR process was strongly inhibited on the Cl^--adsorbed (100) surface, with a B value of $\sim 3.5 \times 10^{-2}$ mA $rpm^{-0.5}$, corresponding to a 3.5 e^- reduction pathway (Fig. 3d). Mukerjee *et al.* also reported that the Pt–Cl interaction on more open facets (*e.g.* Pt(100)) and lower coordination facets (*e.g.* corner and edge) are stronger than those on the Pt(111) facet, which greatly affects the O–O bond breaking.[32] Obviously, the chloride-poisoning resistance of noble-metal-based electrocatalysts such as Pt can be efficiently improved by exposing specific facets that possess weaker interaction with Cl^-.

Another strategy for improving noble-metal-based electrocatalysts in chloride-containing electrolytes is the use of functionalized supports by which means the stability can be significantly improved. Rangel *et al.* reported that depositing Pt on 4-aminobenzenesulfonic acid-functionalized carbon (Pt/C_ABSA) greatly increased its resistance to Cl^- compared with commercial Pt/C (Pt/C_COM).[59] Because of the strong retardation effect of the adsorbed Cl^-, the formation of Pt surface oxides was suppressed followed by a quasi-linear current increase attributed to Pt dissolution. When compared with the cyclic voltammetry (CV) profile of Pt/C_ABSA in a 0.5 M H_2SO_4 electrolyte (activation), adding 5 mM NaCl to the electrolyte (chloride effect) resulted in a weakened oxide reduction peak at around 0.5 V *vs.* Ag/AgCl, as evidenced in the cathodic sweep (Fig. 3e). And the CV profile soon recovered when conducted again in the Cl^--free electrolyte (reactivation). However, the loss of electrochemically active surface area was negligible for Pt/C_ABSA (0.26%) after exposure to 5 mM Cl^-, yet Pt/C_COM showed an obvious loss of 7.83%.

Moreover, it was found that the average Pt particle size of Pt/C_ABSA (4.1 nm) did not change significantly after cycling in an electrolyte containing 25 mM NaCl, while that of Pt/C_COM grew from 2.7 to 3.2 nm with obvious dissolution and recrystallization behavior (Fig. 3f). These demonstrate the excellent stability of Pt electrocatalysts supported on surface-functionalized carbon in chloride-containing electrolytes. Another typical example is the Rh_xS_y electrocatalysts, where a series of studies indicated that their stability against Cl^- poisoning can be significantly enhanced after being supported on carbon nanotubes.[67–69]

In summary, regarding the ORR process in chloride-containing electrolytes, developing noble-metal-free, especially metal-free, electrocatalysts, such as nitrogen-doped carbon, is a preferred strategy to circumvent the inhibition behavior originating from Cl^- poisoning, because of their high intrinsic resistance. On the other hand, the activity of noble-metal-based electrocatalysts such as Pt can be optimized by tuning the crystal structural sensitivity, so that the Cl^- blocking effect and undesirable H_2O_2 formation are alleviated on high coordination sites. Meanwhile, their stability in chloride-containing electrolytes can be improved through loading on functionalized supports.

3.2. Chloride-resistant OER electrocatalysts

For a rechargeable seawater-based metal–air battery, the charge process relies on the OER electrocatalysis in the air electrode, which is generally considered the rate-limiting step.[70–72] Its main challenge is the chlorine oxidation reactions (HCFR/ClER) that compete with OER, together with the electrocatalyst corrosion phenomenon. Accordingly, multiple strategies have been proposed to obtain highly selective and stable OER electrocatalysts under a chloride-containing environment, such as utilizing the intrinsic OER selectivity criteria, fabricating an inert chloride-retarding layer, or decorating with an anion-rich surface.

Strasser and co-worker summarized the design criteria of OER electrocatalysts for alkaline chloride-containing electrolytes and concluded that those sustaining an overpotential of <480 mV can obtain high oxygen/chlorine selectivity in theory.[27] The activity and stability of electrocatalysts following this criterion would not be compromised in the presence of Cl^-. For instance, Fig. 4a shows the OER activity of NiFe layered double hydroxide (NiFe-LDH) nanoplate electrocatalysts in alkaline (0.1 M KOH, pH = 13) and near-neutral electrolytes (0.3 M borate buffer, pH = 9.2) with/without 0.5 M NaCl as an additive. Obviously, the OER process occurred at a more positive overpotential as the pH decreased from 13 to 9.2. NiFe-LDH satisfied the above criterion at pH = 13, that Cl^- did not adversely affect its OER activity to render an almost unchanged overpotential of ~ 360 mV at a current density of 10 mA cm^{-2}. It even appeared to slightly boost OER activity at pH = 9.2, but whether this could be attributed to molecular oxygen evolution is unclear. Moreover, within the 480 mV overpotential limit of oxygen-selectivity, the faradaic efficiencies of

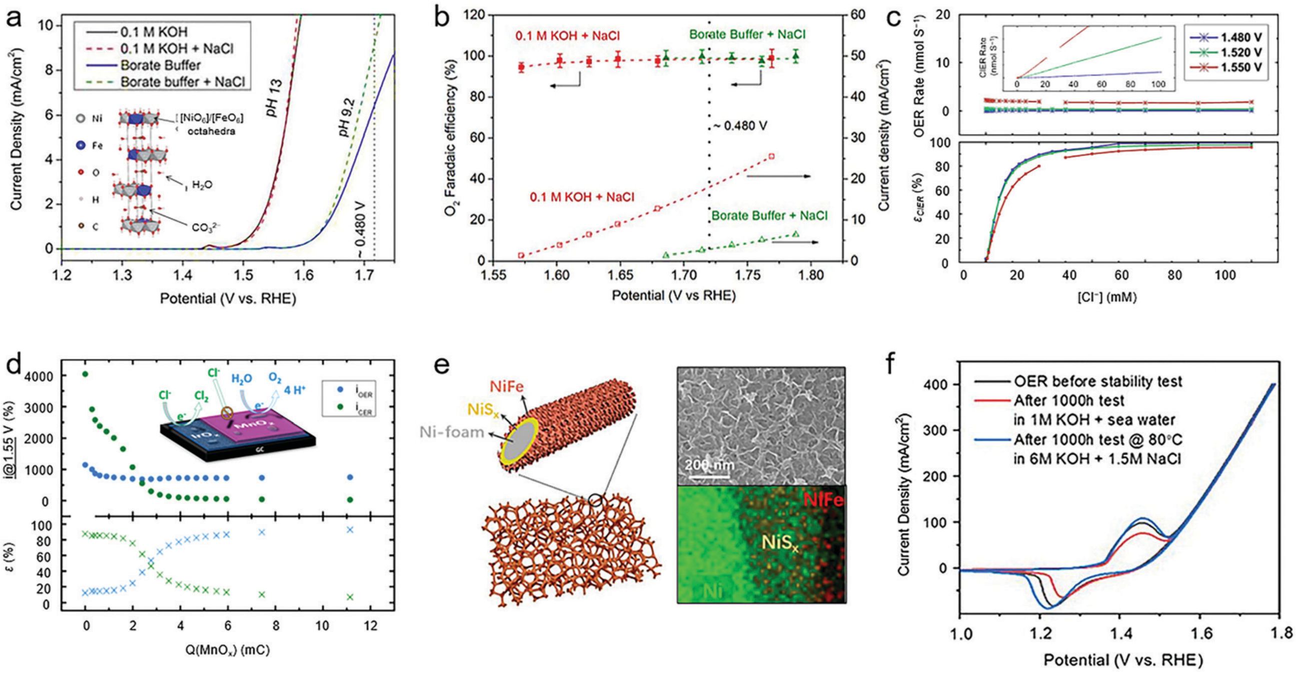

Fig. 4 Chloride-resistant OER electrocatalysts. (a) The OER polarization curves of NiFe-LDH nanoplate electrocatalysts in four different electrolytes (inset: the structural model of NiFe-LDH).[27] (b) The faradaic efficiency and current density of NiFe-LDH as a function of potential.[27] Copyright 2016, Wiley-VCH. (c) Plots of the OER and ClER reaction rates and selectivity of IrO_x electrocatalysts as a function of the Cl^- concentration at various disk potentials.[73] Copyright 2018, Elsevier. (d) Currents and corresponding selectivity for the OER and ClER of MnO_x/IrO_x electrocatalysts at E = 1.55 V as a function of the charge ascribed to the MnO_x layer, $Q(MnO_x)$ (inset: a sketch of the MnO_x/IrO_x deposition structure, which inhibits the ClER *via* blocking Cl^- from reaching IrO_x underneath).[26] Copyright 2018, American Chemical Society. (e) A schematic illustration, a scanning electron microscopy (SEM) image, and elemental mapping of the 3D multilayer NiFe/NiS_x–Ni electrocatalyst.[50] (f) CV curves of NiFe/NiS_x–Ni before and after 1000 h of water splitting in an alkaline simulated-seawater electrolyte.[50] Copyright 2019, PNAS.

NiFe-LDH electrocatalysts toward OER remained at more than 95% at both pH values, either with or without NaCl (Fig. 4b). When compared with the OER selectivity, the difference in longer-term stability in various electrolytes is more obvious. NiFe-LDH could operate stably for two hours in alkaline electrolytes regardless of whether Cl^- was introduced; in contrast, its stability in near-neutral electrolytes became much worse in the presence of Cl^-, where the potential sustaining 10 mA cm^{-2} increased sharply to 2.4 V accompanied by an undesirable HCFR process.[72] Therefore, it is inferred that OER electrocatalysts with no less activity than NiFe-LDH can operate in a chloride-containing electrolyte, but usually require a relatively high pH and a moderate current density.

Compared with alkaline conditions where quite a few electrocatalysts are applicable, realizing the OER process in an acid chloride-containing electrolyte is more challenging because most of the noble-metal-free electrocatalysts suffer from easy degradation in acid media, and the OER selective potential range is narrow, reducing its thermodynamic advantages over ClER (Fig. 2c). Thus, noble-metal-based OER electrocatalysts (*e.g.*, Ir-based or Ru-based electrocatalysts) should be preferred with regard to their high intrinsic OER activity, but with the vast majority of them it has proven difficult to achieve desired selectivity toward OER over ClER.[74–77] Koper *et al.* used a rotating ring disk electrode method to study the ClER behavior of amorphous IrO_x, which has long been regarded as an active and stable OER electrocatalyst.[73] Fig. 4c shows the plots of OER and ClER reaction rates as a function of Cl^- concentration in 0.5 M $KHSO_4$. The three disk potentials of 1.480, 1.520, and 1.550 V correspond to three regimes where only ClER is present, ClER is major but OER is minor, and both ClER and OER are present, respectively. The faradaic efficiency of ClER (ε_{ClER}) rose and converged to above 90% as the Cl^- concentration increased to 0.1 M regardless of potential. Unexpectedly, this work suggested that OER and ClER proceed independently, which contradicts the scaling relationship reported in other literature.[43–45] On the other hand, manganese oxide (MnO_x) as a noble-metal-free OER/ClER selective electrocatalyst has received great interest.[78–80] Bennett *et al.* reported an MnO_x-based electrocatalyst with high selectivity toward OER in acid seawater for the first time.[81] More importantly, MnO_x can remain moderately stable in the acid OER process, in contrast to many noble-metal-free electrocatalysts, such as CoO_x, NiFe-LDH, and other double hydroxides.[72,82–86] Nevertheless, the mechanism by which MnO_x has high selectivity has not been clear up to now, and relevant investigations would gain insight into the design of highly selective OER electrocatalysts under a chloride environment and therefore should be seriously considered.

For those OER electrocatalysts with inherently poor selectivity, such as IrO_x, ingenious composite structural design becomes necessary: for example, fabricating an inert chloride-retarding layer on the electrocatalyst surface. Koper and co-workers *in situ* electrodeposited a thin MnO_x film ($\sim$5–20 nm) on glassy carbon (GC)-supported hydrous IrO_x.[26] The selectivity of pristine IrO_x toward OER was as low as 14% at 1.55 V, in the presence of 0.03 M Cl^- at pH = 0.88. However, after covering it with an MnO_x layer with a certain thickness, >90% OER selectivity was obtained from the modified IrO_x despite a moderate drop in activity, to afford a highly OER-selective electrocatalyst instead of a ClER electrocatalyst (Fig. 4d). The MnO_x layer benefitted the selective formation of O_2 over Cl_2. In contrast with the above study, as an electrocatalytically active phase, in this work MnO_x was found to be not highly OER-active in strongly acid conditions within the potential window used.[80,86–88] On the one hand, the porous amorphous MnO_x layer allows easy transfer of H_2O, O_2, and H^+ between the electrolyte and IrO_x.[89–93] On the other hand, it decreases the ClER selectivity by disfavoring Cl^- transport, owing to the buried interfaces resulting from concentration polarization, as reported recently by Takanabe *et al.*[94,95] Thus, the selective chloride-retarding layer can solely inhibit ClER whereas OER remains relatively unaffected. Similarly, Hashimoto's group deposited a series of Mn-based mixed oxides on the IrO_x substrate, which exhibited excellent OER selectivity under various conditions.[96–98] For example, Ti-supported IrO_x was coated with heterometal-doped MnO_x to achieve OER-selectivity in an analogous fashion, when different dopants have considerable influence on the stability and morphology of the modified MnO_x layer. Ravichandran *et al.* also demonstrated selective retardation of Cl^- in seawater OER electrolysis.[99] Besides enhanced OER selectivity over competitive ClER, the inert chloride-retarding layer strategy also efficiently prevents the inner electrocatalytic active phase from corrosion in acid chloride-containing electrolytes.[26]

Another effective strategy is to decorate the electrocatalyst surface with cation-selective polyanions, which can simultaneously enhance OER selectivity and corrosion resistance by repelling Cl^-.[100,101] As shown in Fig. 4e, Dai *et al.* reported a multilayer OER electrocatalyst composed of an NiFe/NiS_x bilayer fabricated on porous Ni foam (NiFe/NiS_x–Ni).[50] Upon activation in alkaline conditions, negatively charged sulfate polyanions derived from the anodic process of the underlying NiS_x layer were decorated on NiFe/NiS_x–Ni. After 1000 h of splitting in an alkaline simulated seawater electrolyte (1 M KOH + 0.5 M NaCl), CV curves of the NiFe/NiS_x–Ni anode showed an overpotential of 510 mV (without iR compensation) at a current density as high as 400 mA cm^{-2}, which decreased to $\sim$300 mV after iR compensation and was far below the 490 mV overpotential limit that would trigger HCFR (Fig. 4f). The polyanion-passivated Ni^{3+} layers inhibited the corrosion on the electrocatalyst structure by repelling Cl^-. Mass spectrometry results revealed no anodic chlorine evolution while gas chromatography results rendered a near 100% faradaic efficiency of O_2 production, verifying an excellent OER selectivity. Obviously, the anion-rich surface strategy simultaneously endows the NiFe/NiS_x–Ni electrocatalyst with good activity, selectivity, and corrosion resistance in chloride-containing electrolytes.

In summary, regarding the OER process, electrocatalysts possessing relatively low overpotentials (<490 mV, *e.g.*, NiFe-LDH) can operate in an alkaline chloride-containing electrolyte with satisfactory selectivity toward OER over HCFR. In acid conditions, although most of the existing electrocatalysts hardly achieve the desired selectivity, manganese oxides still demonstrate considerable OER-selective activity. Moreover, it can also function as an inert chloride-retarding layer to integrate with conventional OER-active electrocatalysts to obtain excellent selectivity and corrosion resistance in chloride-containing electrolytes. Similarly, the anion-rich decorated surface strategy also efficiently alleviates these issues.

3.3. Electrocatalysts applicable to seawater-based electrolytes

Direct implementation of natural seawater in electrocatalytic processes is of more significance for seawater-based metal–air batteries than for chloride-containing electrolytes, which raises a higher requirement for robust and efficient electrocatalysts. Previously, although most relevant work was centered on water electrolysis rather than the battery field, it has important implications for promoting the OER process in seawater.[102–106] Beyond Cl^-, on the one hand, the influence of other dissolved ions, such as Na^+ and SO_4^{2-}, in seawater on the ORR/OER electrocatalytic processes at the cathode was negligible due to intrinsic inertness or low concentration.[31] But for the seawater-based Na–air batteries, Na^+ plays a significant role in the anodic processes based on redox reactions of Na/Na^+ extracted from/released to seawater.[13] On the other hand, the formation of insoluble precipitates (*e.g.*, magnesium hydroxide in alkaline conditions) as well as particulates and microorganisms originating from natural seawater may cover the electrode surface, bury the active sites, and reduce the electrochemically active surface area.[27] Thus, to alleviate this problem, not only are design strategies necessary for chloride-resistant electrocatalysts, but large-specific-surface electrocatalysts with an increased number of active sites and rapid charge transfer are favorable, which can be realized by elaborate structural design, such as a multilayer or core–shell structure supported on a 3D porous substrate.

The above discussed multilayer NiFe/NiS_x–Ni integrated structure was tested as an anode for seawater electrolysis by pairing it with an Ni–NiO–Cr_2O_3 cathode.[50] The electrolyzer could operate with a current density of 400 mA cm^{-2} at 2.12 and 2.02 V in an alkaline natural seawater electrolyte (1 M KOH in seawater) and simulated seawater electrolyte (1 M KOH + 1.5 M NaCl), respectively, for over 1000 h without obvious decay, which was also corroborated by the above three-electrode measurements. Similarly, Kim *et al.* developed carbon-coated $Na_2Co_{1-x}Fe_xP_2O_7$ ($0 \leq x \leq 1$) nanoparticles supported on a carbon cloth (NCFPO/C@CC) as an OER electrocatalyst, whose activity could be optimized by controlling the Co/Fe ratio (Fig. 5a).[107] It operated well in an alkaline simulated seawater electrolyte (0.1 M KOH + 0.5 M NaCl), showing an overpotential of 285 mV at a current density of 10 mA cm^{-2} as well as long-term durability over 100 h, without the generation of reactive chloride species. And in an alkaline seawater electrolyte (KOH in seawater, pH = 12.7), only a slight increase (40 mV) in overpotential was observed. Thus, the self-supporting multilayer structure helps to achieve superior OER activity and durability in alkaline seawater electrolytes.

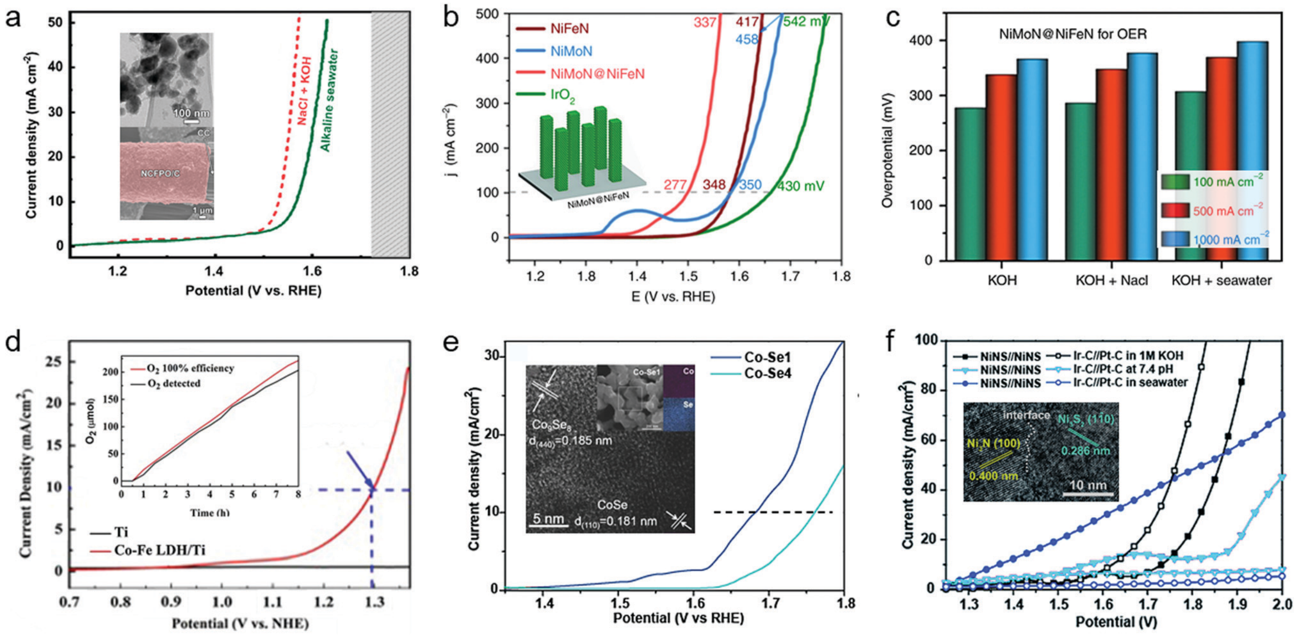

Fig. 5 Seawater-applicable electrocatalysts. (a) The OER polarization curves of NCFPO/C@CC in alkaline simulated-seawater (0.1 M KOH + 0.5 M NaCl) and real seawater (KOH in seawater, pH = 12.7) electrolytes (inset: TEM and SEM images of NCFPO/C@CC).[107] Copyright 2020, American Chemical Society. (b) The OER polarization curves of different electrocatalysts in 1.0 M KOH (inset: a schematic illustration of 3D self-supported core–shell NiMoN@NiFeN).[111] (c) The overpotentials of NiMoN@NiFeN at current densities of 100, 500, and 1000 mA cm^{-2} in alkaline conventional (KOH), simulated seawater (KOH + NaCl), and real seawater (KOH + seawater) electrolytes.[111] Copyright 2019, Springer Nature. (d) The OER polarization curves of Co–Fe LDH/Ti in seawater (inset: the faradaic efficiency for the simultaneous detection of dissolved O_2).[112] Copyright 2017, Elsevier. (e) The OER polarization curves of Co–Se1 and Co–Se4 in seawater (inset: high-resolution TEM images, an SEM image, and elemental mapping of Co–Se1).[113] Copyright 2018, Wiley-VCH. (f) Polarization curves of NiNS//NiNS and Ir–C//Pt–C overall water splitting systems in 1.0 M KOH, buffer solution (pH = 7.4), and seawater (inset: a high-resolution TEM image of NiNS).[114] Copyright 2019, Royal Society of Chemistry.

A self-supporting core–shell structure is another promising solution for electrocatalysts applicable to seawater-based electrolytes. Transition metal nitrides are efficient OER electrocatalysts due to their high corrosion resistance, electronic conductivity, and mechanical strength.[108–110] Yu *et al.* reported a 3D core–shell OER electrocatalyst for alkaline seawater electrolysis, in which uniform NiFeN nanoparticles were fabricated on NiMoN nanorods self-supported on porous Ni foam (NiMoN@NiFeN).[111] When evaluated in 1 M KOH, NiMoN@NiFeN achieved high current densities of 100 and 500 mA cm^{-2} with overpotentials of 277 and 337 mV, respectively, which were considerably smaller than those of single-layer NiFeN, NiMoN, and noble-metal-based IrO_2 electrocatalysts (Fig. 5b). In an alkaline simulated seawater electrolyte (1 M KOH + 0.5 M NaCl) and real seawater electrolyte (1M KOH in seawater), its OER activity showed only slight decay (Fig. 5c). Even at 1000 mA cm^{-2}, the required overpotential of 398 mV is still below the 490 mV overpotential limit, with excellent selective OER in seawater. On the one hand, the 3D core–shell structure with multiple porosity is beneficial for constructing abundant active sites and accelerated reactant/product diffusion. On the other hand, the outer NiFeN nanoparticles would be *in situ* converted into an NiFe oxide/hydroxide amorphous layer during the OER process, which is favorable for OER selectivity and corrosion resistance to Cl^-.

Besides alkaline seawater-based electrolytes, researchers also studied the possibility of using neutral natural seawater electrolytes without additives. Chen *et al.* synthesized Co–Fe layered double hydroxide nanoparticles supported on a Ti mesh (Co–Fe LDH/Ti) as an OER electrocatalyst for direct seawater oxidation.[112] As shown in Fig. 5d, it required an overpotential of 530 mV to achieve a current density of 10 mA cm^{-2} in seawater at pH = 8. Although exceeding the 490 mV overpotential limit, a faradaic efficiency of $\sim$94% was still obtained at a constant overpotential of 560 mV, rendering good selectivity toward OER over HCFR. However, this indicates that the electrocatalytic process in neutral seawater is more challenging.

Further enhancing the intrinsic electrocatalytic efficiency of active sites can also compensate for these disadvantages to some extent. For example, when compared with common single-component electrocatalysts, fabricating heterogeneous structures through charge state or interfacial manipulation usually delivers superior electrocatalytic efficiency, which is more desirable for the real seawater process that involves the burying effect and complex side reactions. Qiao *et al.* developed a series of 3D self-supporting cobalt selenide electrocatalysts consisting of CoSe and Co_9Se_8 phases, while the Co^{3+}/Co^{2+} charge ratio could be manipulated.[113] Fig. 5e shows the OER activity of two cobalt selenide samples in seawater, where Co–Se1 with a higher Co charge state demonstrates superior electrocatalytic activity.[115,116] By integrating Co–Se1 and Co–Se4 (with a lower Co charge and better HER activity) as the anode and cathode of an electrolyzer, respectively, a current density of 10.3 mA cm^{-2} was achieved at 1.8 V for overall water splitting in neutral natural seawater without adding alkali, much higher than that of the Ir–C//Pt–C electrolyzer (2.9 mA cm^{-2}). Qiao's group further synthesized a 3D nickel nitride/sulfide (NiNS) electrocatalyst supported on Ni foam, in which the Ni_3N/Ni_3S_2 phase interface functioned as efficient active sites conducive to dissociative adsorption of water molecules (Fig. 5f).[114] When applied as both the anode and cathode for overall seawater splitting, a higher current density of 48.3 mA cm^{-2} could be achieved at 1.8 V. The 3D self-supporting network together with elaborate electronic or interfacial manipulation are responsible for the excellent OER activity of these heterostructure electrocatalysts in seawater.

In order to obtain satisfactory electrocatalytic processes in seawater-based electrolytes, attention should be paid to the electrode structure design to expose more active sites and accelerate mass/charge transfer, beyond these design strategies for chloride-resistant electrocatalysts. 3D hierarchical self-supporting structures with plentiful electrocatalytic centers and rapid charge transfer are particularly favorable, such as multilayer or core–shell integrated structures. Besides, for applications in neutral seawater, further improvement in the efficiency of active sites plays a significant auxiliary function, while the optimal manipulation of heterogeneous structures in terms of charge state or interface is helpful.

4. Seawater-based metal–air batteries

4.1. Development history of seawater-based metal–air batteries

As shown in Fig. 6, a brief timeline summarizes the development of seawater-based metal–air batteries, accompanied by other relevant battery systems. Since the 1940s, seawater as an electrolyte has been employed in some battery prototypes, and Mg (anode)–AgCl (cathode) batteries were the first commercial primary batteries using seawater electrolytes, which were produced for military applications.[117] Since then, more cathode materials, including chlorides and iodides such as CuCl,[118] $PbCl_2$,[119] Hg_2Cl_2,[120] and CuI,[121] were successively produced and applied, considering their advantages of low cost, low hygroscopicity, and high chemical stability.

As the object of this review, a few metal–air batteries using seawater electrolytes were first developed around the 1990s, which operated long-term in the subsea environment *via* a primary battery mode and demonstrated superior potential for industrial applications.[11,12,122–125] The ORR process occurred using dissolved O_2 as the cathode oxidant, while Mg, Al, and their alloys were studied as possible anode materials. For example, in 1994 Shen *et al.* fabricated Al–air batteries using Al alloy as the anode, natural seawater as the electrolyte, and Teflon-bonded Co_3O_4/C as the cathode electrocatalysts together with dissolved oxygen as the cathode oxidant, which delivered a low current density of $\sim$0.1 mA cm^{-2} at 1.4 V due to the limited solubility of O_2 in seawater.[123] It was found that the Teflon-bonded Co_3O_4/C was almost as active as the Pt/C electrocatalysts, while a long-term test in Brightlingsea Harbour, Essex showed quite stable battery performance over 70 days. A conceptual battery design suggested an energy density of 1008 W h kg^{-1}, significantly higher than that for other conventional primary batteries for subsea use.

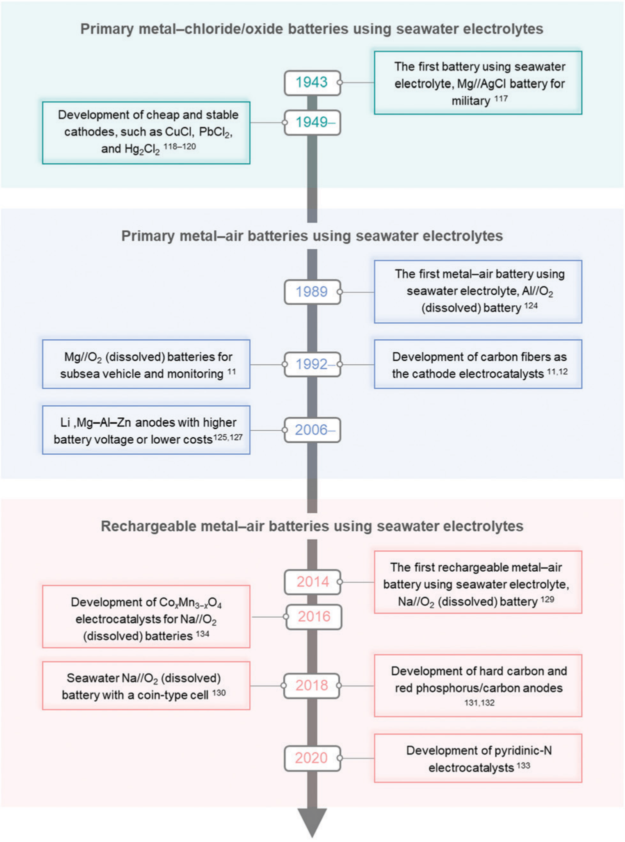

Fig. 6 A brief timeline summarizing the development history of seawater-based metal–air batteries, accompanied by other relevant battery systems.

Stable electric power is a major difficulty for long-term operation in the ocean, where high-capacity and slow-discharge batteries using seawater-based electrolytes are desirable.[126] In 2000, a seawater-based metal–air battery system was developed for a sea-floor borehole seismic observatory that was installed in the north-western Pacific basin. It mainly consisted of four Mg–air batteries using seawater as the electrolyte and dissolved O_2 as the cathodic oxidant, a power control system, a DC/DC converter, a data logger, and an accumulator (Fig. 7a).[12] This battery delivered a cell voltage of ~1.6 V by using a replaceable magnesium alloy rod as the anode and carbon fibers supported by a titanium frame as the cathode. It continuously generated an average of 6 W power for 5 years, while the estimated energy density of 318 W h kg^{-1} was even higher than those of LIBs now in use. Earlier in 1997, operating in a similar mode and with similar electrode materials, a seawater-based Mg–air battery powered the autonomous control system of a subsea well in the Ionian Sea.[11] Its mean power in the no-activity mode was 8 W, which increased to as much as 35 W under monitoring of the well. Attributed to the stable environment but low oxygen content in the subsea environment, the above metal–air batteries usually possessed relatively large capacity but low power density. Another important characteristic is that the seawater as electrolyte needs to flow through the electrodes continuously, to supply the cathodes with oxygen and take away the sediments generated on the anodes, and thus the cell configurations are usually open.

To increase the cell voltage and solve the electrode blockage issue, more active metal anodes were subsequently applied. Primary seawater-based Li–air batteries were designed using a protected lithium electrode as the anode and oxygen dissolved in seawater as the oxidant, which enabled a higher cell voltage of 3 V.[127,128] To realize electrical energy storage and supply, Kim *et al.* further successfully developed a series of rechargeable Na–air batteries using seawater as the electrolyte, which operated based on the redox reactions of Na/Na$^+$ extracted from/released to seawater at the anode, combined with ORR/OER of dissolved O_2 at the cathode.[129] Na metal anodes had to be submerged in non-aqueous anolytes and separated from seawater by Na-ion conducting membranes which also served as solid electrolytes, while the cathodes were in contact with seawater. Various cathode electrocatalysts, anode materials, and cell configurations have been developed.[29,129–133] Fig. 7b shows the charge–discharge voltage profiles of a seawater-based Na–air battery using porous $Co_xMn_{3-x}O_4$ (CMO) nanoparticles as the bifunctional electrocatalyst in the cathode, which gave rise to a much smaller voltage gap and superior stability compared to noble-metal-based Pt/C and Ir/C electrocatalysts.[134] However, these existing alkali seawater-based metal–air batteries may suffer from poor anodic stability due to the intrinsic high reactivity of alkali metals.

Consequently, satisfactory durability and cell voltage are difficult to achieve simultaneously for these existing seawater-based metal–air battery prototypes, and the best selection of battery systems should keep a delicate balance regarding the occasions on which they are applied. It is worth noting that most previous battery prototypes still used common cathode electrocatalysts designed for conventional electrolytes, such as carbon fibers and transition metal oxides. For improved performance, attention should be paid to optimization of electrocatalysts according to the seawater-based electrolyte.

4.2. Potential application occasions

Benefitting from the use of seawater-based electrolytes and the inherent advantages of metal–air batteries, seawater-based metal–air batteries will be suitable power sources and energy storage devices in diverse environments, including islands, marine environments, and the ocean, in the future, far beyond subsea applications. From the aspect of power, their potential applications can be divided into three categories: small, medium, and large, as illustrated in Fig. 7c.[13]

On the one hand, some small-power seawater-based metal–air battery prototypes have been used in subsea observations, as discussed above. On the other hand, future small-power seawater-based metal–air batteries are also applicable for extreme environments, such as marine navigation and salvage fields, including buoys and life jackets. One key advantage is that the inactivated batteries can be stored for a long time in dry conditions before use, and can soon be activated by injection of or immersion in seawater to power key devices, such as light-emitting diode (LED) lamps or a global positioning system (GPS) or to provide heat preservation. For example, when a drowning person wears a life jacket immersed in seawater, the equipped small-power seawater-based metal–air batteries on the jacket

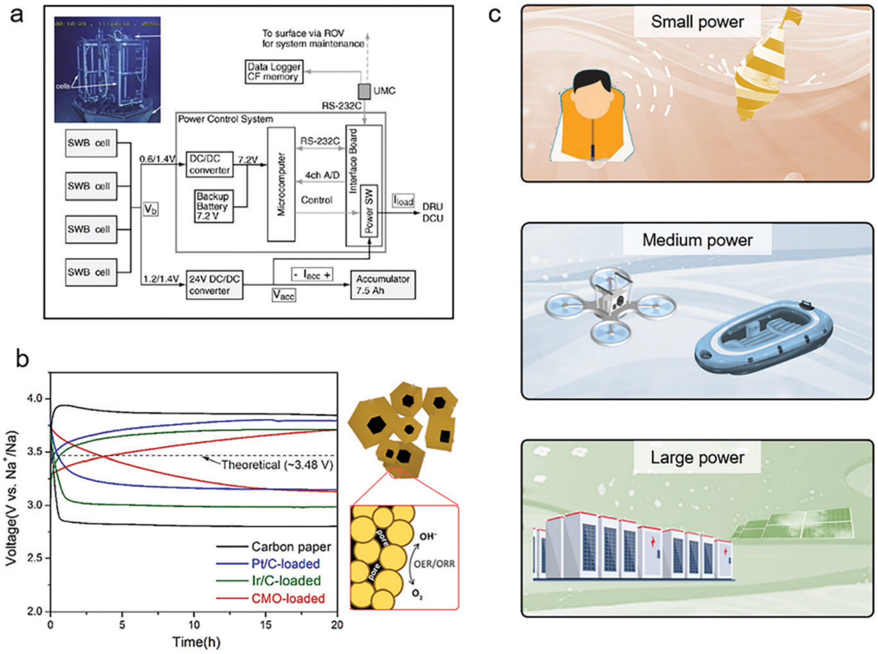

Fig. 7 The development history and applications of seawater-based metal–air batteries. (a) A schematic diagram of a seawater-based metal–air battery (SWB) system for a borehole broadband seismic observatory on the sea floor (inset: photograph).[12] Copyright 2009, Elsevier. (b) The charge–discharge voltage profiles of seawater-based Na–air batteries with different cathode electrocatalysts, accompanied by a schematic illustration of the porous CMO electrocatalyst.[134] Copyright 2016, American Chemical Society. (c) Potential applications of seawater-based metal–air batteries in terms of power.

could help to keep the body warm, sound an alarm to call for help, or drive the GPS to send real-time location information. They are also targeted for more reliable marine navigation by replacing existing small-power sources based on LIBs or nickel-metal hydride batteries. Medium-power applications are expected to provide power for a wide number of fields, including military (*e.g.*, exploratory drones), civil (*e.g.*, yachts), scientific (*e.g.*, subsea exploration), and industrial (*e.g.*, offshore well) applications; in particular, in small navigation and aviation machines, which play an important role in maritime search and rescue and photography. The use of seawater-based metal–air batteries can greatly reduce operational costs and enhance the system energy density, which are targeted for replacing the existing medium-power sources based on internal combustion engines or LIBs. Large-power seawater-based metal–air batteries aim at serving as large-scale and stationary energy storage systems on islands or areas adjacent to the ocean, to store electrical energy intermittently generated from tidal power stations, solar panels, hydro-turbines, *etc.*, which are of importance for industrial and military applications.

5. Summary and outlook

As freshwater is becoming a more and more precious resource, metal–air batteries exploiting seawater-based electrolytes can store/provide electrical energy to meet the demands in broader application areas, reduce battery costs, and alleviate competition with the use of fresh water. However, applicable ORR/OER electrocatalysts in air electrodes should be distinct from those for existing conventional metal–air batteries due to the influence of seawater components on the electrocatalytic processes. Although both ORR and OER are thermodynamically favorable in seawater, the kinetic factors are more complicated. A better understanding of the relevant influence mechanisms prompts the development of strategies for enhancing the resistance of electrocatalysts to the seawater environment.

Concerning the ORR process under a chloride-containing environment, the strong adsorption of Cl^- on electrocatalysts blocks a large fraction of active sites and induces a two-electron ORR pathway, especially for noble-metal-based electrocatalysts, while metal-free electrocatalysts, such as N-doped carbon, can efficiently resist the Cl^- poisoning effect. Meanwhile, the activity and stability of noble-metal-based electrocatalysts can be improved by structural regulation, including exposing selected surfaces and employing functionalized supports. For the OER process, the oxidation of Cl^- competes with OER because of its kinetically favorable two-electron pathway, together with chloride-induced electrocatalyst corrosion as another challenge. In alkaline conditions, OER electrocatalysts with low overpotentials ($<$490 mV) can possibly operate with satisfactory selectivity toward OER over HCFR; in acid conditions, manganese oxides possess considerable intrinsic OER selectivity and stability compared with the vast majority of other electrocatalysts. Moreover, fabricating an inert chloride-retarding layer or an anion-rich decoration layer can efficiently address the selectivity and corrosion issues. Compared with chloride-containing electrolytes, the electrocatalytic processes in real seawater suffer from additional problems, such as the formation of insoluble precipitates on the electrode surface. In addition to the strategies for chloride-resistant

ORR/OER electrocatalysts, 3D hierarchical self-supporting structures are favorable due to abundant exposed active sites and accelerated charge transfer. Meanwhile, further improving the electrocatalyst efficiency *via* heterogeneous structure manipulation of the charge state or interface benefits their applications in seawater-based electrolyte.

In general, developing efficient electrocatalysts for seawater-based metal–air batteries should focus on both aspects of intrinsic performance and multiscale structural regulation. Concerning the intrinsic performance, various electrocatalyst materials, such as noble-metal-based, noble-metal-free, and metal-free materials possess completely distinct ORR/OER activity, selectivity, and stability in the presence of chloride ions. And the intrinsic electrocatalytic ability can be further improved by tuning the electronic structure and atomic-scale surface/interface structure. More importantly, to overcome the more complex seawater environment, combining various componential and structural strategies at the multiscale has become the dominant tendency, such as employing functionalized supports/coating layers/charge decorating layers or fabricating 3D integrated electrodes, together with various targeted electrocatalyst components. Although a few seawater-based metal–air batteries have been developed with practical industrial applications, it is found that those limited battery prototypes still relied on conventional electrocatalysts which lack corresponding optimization for seawater-based electrolytes. Finally, potential applications in terms of power are proposed for future seawater-based metal–air batteries, which are expected to compete with widely-used energy technologies like LIBs in marine, underwater, and offshore power applications.

The unlimited supply of seawater on Earth makes the seawater-based metal–air battery an increasingly attractive next-generation energy conversion and storage technology with environmental friendliness. It shows great potential but also faces multiple challenges compared to conventional metal–air batteries. First, air electrode electrocatalysts should be rationally designed in accord with the practical demands of seawater-based electrolytes. The core scientific challenge is an in-depth study of the influence mechanisms of chloride ions on electrocatalysts during the ORR and OER processes: for example, the special adsorption inhibition and competitive inhibition on various active sites, such as noble metal atoms, transition metal atoms, and carbon/nitrogen atoms. Based on these perceptions, some emerging electronic and atomic-scale methods, including anion/cation regulation,[21,135] defect engineering,[22,24,136] and phase tailoring.[137] may be helpful for enhancing chloride-resistance. Subsequently, robust ORR/OER bifunctional electrocatalysts applicable to real seawater-based electrolytes should focus not only on the inhibition of undesirable electrochemical and chemical processes originating from the seawater components, but also on the enhancement of cathode utilization. Exploring multiscale structural strategies to construct a highly active electrode surface with more exposed active sites and accelerated mass transfer is highly promising, when many typical electrocatalyst and electrode designs can be used.[16,20]

Besides the air cathode, the metal anode also plays a critical role in a metal–air battery. On the one hand, relatively inactive metals such as Mg and Al usually suffer from electrode blockage due to hydroxide precipitates and low operating voltages, and are thus usually used in a primary battery mode.[138] Moreover, the chloride environment in seawater will accelerate anode corrosion, where strategies such as 3D surface structure and surface coating are promising.[139,140] On the other hand, the key issue for highly active metals such as Na and Li is their highly-reactive nature in aqueous electrolyte. They are usually unstable and supposed to be separated from the aqueous electrolyte. Therefore, usage of an intercalation-type or alloying-type anode instead of metal anodes is preferred, and a non-aqueous anolyte is preferred and should be separated from the seawater-based catholyte by a cation-conducting membrane.[129] For example, Kim's group has developed efficient selective Na-ion conducting membranes based on NASICON ($Na_{1+x}Zr_2Si_xP_{3-x}O_{12}$, $0 < x < 3$), which worked well in a series of rechargeable batteries with Na-based anodes.[29,129,141,142] In general, membranes with high cation conductivity and selectivity, high electrochemical and chemical stability, and enough mechanical strength are desirable in practical applications.

Furthermore, at a holistic level, battery configuration optimization on various compartments, including electrolytes, air cathodes, and metal anodes, should be a critical engineering challenge for promoting the energy/power density and durability of seawater-based metal–air batteries, where advanced nanotechnologies such as 3D printing can be applied to the fabrication of electrodes.

It is believed that new insights for promoting the ORR/OER electrocatalytic processes in chloride-containing and seawater electrolytes will lay the foundation for designing metal–air batteries using seawater-based electrolytes, from both the perspectives of theoretical research and technological applications. Although there considerable advances exist relation to the design of electrocatalysts and the fabrication of battery prototypes with considerable electrochemical performance, many issues still need to be resolved before commercial applications are realized. Facing both opportunities and challenges, seawater-based metal–air batteries are expected to play a significant role in a wide number of applications and to contribute to clean energy systems in a future fossil-fuel-free society. Moreover, relevant electrocatalyst strategies and methodologies for such complex seawater systems could potentially inspire other electrochemical energy technologies.

Conflicts of interest

There are no conflicts to declare.

Acknowledgements

This work was supported by the National Natural Science Foundation of China (21825501, 21905157, and U1801257), the National Key Research and Development Program (2016YFA0202500 and 2016YFA0200102), the China Postdoctoral Science Foundation (2019M650697), and the Tsinghua University Initiative Scientific Research Program.

References

1 S. Chu and A. Majumdar, *Nature*, 2012, **488**, 294–303.

2 J. Fu, Z. P. Cano, M. G. Park, A. P. Yu, M. Fowler and Z. W. Chen, *Adv. Mater.*, 2017, **29**, 1805230.

3 B. Chen, D. L. Chao, E. Z. Liu, M. Jaroniec, N. Q. Zhao and S. Z. Qiao, *Energy Environ. Sci.*, 2020, **13**, 1096–1131.

4 V. Aravindan, Y. S. Lee and S. Madhavi, *Adv. Energy Mater.*, 2015, **5**, 1402225.

5 J. Pan, Y. Y. Xu, H. Yang, Z. H. Dong, H. F. Liu and B. Y. Xia, *Adv. Sci.*, 2018, **5**, 1700691.

6 J. Yu, B. Q. Li, C. X. Zhao, J. N. Liu and Q. Zhang, *Adv. Mater.*, 2020, **32**, 1908488.

7 S. Fukuzumi, Y. M. Lee and W. Nam, *ChemSusChem*, 2017, **10**, 4264–4276.

8 A. A. El-Moneim, N. Kumagai and K. Hashimoto, *Mater. Trans.*, 2009, **50**, 1969–1977.

9 N. Jiang and H. M. Meng, *Surf. Coat. Technol.*, 2012, **206**, 4362–4367.

10 W. J. Luo, Z. S. Yang, Z. S. Li, J. Y. Zhang, J. G. Liu, Z. Y. Zhao, Z. Q. Wang, S. C. Yan, T. Yu and Z. G. Zou, *Energy Environ. Sci.*, 2011, **4**, 4046–4051.

11 O. Hasvold, H. Henriksen, E. Melvaer, G. Citi, B. O. Johansen, T. Kjonigsen and R. Galetti, *J. Power Sources*, 1997, **65**, 253–261.

12 M. Shinohara, E. Araki, M. Mochizuki, T. Kanazawa and K. Suyehiro, *J. Power Sources*, 2009, **187**, 253–260.

13 S. M. Hwang, J. S. Park, Y. Kim, W. Go, J. Han, Y. Kim and Y. Kim, *Adv. Mater.*, 2019, **31**, 1804936.

14 H. F. Wang, C. Tang, B. Wang, B. Q. Li and Q. Zhang, *Adv. Mater.*, 2017, **29**, 1702327.

15 N. T. Suen, S. F. Hung, Q. Quan, N. Zhang, Y. J. Xu and H. M. Chen, *Chem. Soc. Rev.*, 2017, **46**, 337–365.

16 C. Tang, H. F. Wang and Q. Zhang, *Acc. Chem. Res.*, 2018, **51**, 881–889.

17 M. Qiao, C. Tang, L. C. Tanase, C. M. Teodorescu, C. M. Chen, Q. Zhang and M. M. Titirici, *Mater. Horiz.*, 2017, **4**, 895–899.

18 X. L. Tian, X. F. Lu, B. Y. Xia and X. W. Lou, *Joule*, 2020, **4**, 45–68.

19 C. C. Hou, H. F. Wang, C. X. Li and Q. Xu, *Energy Environ. Sci.*, 2020, **13**, 1658–1693.

20 X. S. Wang, A. Vasileff, Y. Jiao, Y. Zheng and S. Z. Qiao, *Adv. Mater.*, 2019, **31**, 1803625.

21 C. X. Zhao, B. Q. Li, M. Zhao, J. N. Liu, L. D. Zhao, X. Chen and Q. Zhang, *Energy Environ. Sci.*, 2020, **13**, 1711–1716.

22 D. H. Li, Y. Jia, G. J. Chang, J. Chen, H. W. Liu, J. C. Wang, Y. F. Hu, Y. Z. Xia, D. J. Yang and X. D. Yao, *Chem*, 2018, **4**, 2345–2356.

23 Y. Jia, L. Z. Zhang, L. Z. Zhuang, H. L. Liu, X. C. Yan, X. Wangl, J. D. Liu, J. C. Wang, Y. R. Zheng, Z. H. Xiao, E. Taran, J. Chen, D. J. Yang, Z. H. Zhu, S. Y. Wang, L. M. Dai and X. D. Yao, *Nat. Catal.*, 2019, **2**, 688–695.

24 Z. H. Xiao, Y. Wang, Y. C. Huang, Z. X. Wei, C. L. Dong, J. M. Ma, S. H. Shen, Y. F. Li and S. Y. Wang, *Energy Environ. Sci.*, 2017, **10**, 2563–2569.

25 V. Stamenkovic, N. M. Markovic and P. N. Ross, *J. Electroanal. Chem.*, 2001, **500**, 44–51.

26 J. G. Vos, T. A. Wezendonk, A. W. Jeremiasse and M. T. M. Koper, *J. Am. Chem. Soc.*, 2018, **140**, 10270–10281.

27 F. Dionigi, T. Reier, Z. Pawolek, M. Gliech and P. Strasser, *ChemSusChem*, 2016, **9**, 962–972.

28 Y. Q. Wang, Y. Q. Zou, L. Tao, Y. Y. Wang, G. Huang, S. Q. Du and S. Wang, *Nano Res.*, 2019, **12**, 2055–2066.

29 J. K. Kim, E. Lee, H. Kim, C. Johnson, J. Cho and Y. Kim, *ChemElectroChem*, 2015, **2**, 328–332.

30 F. L. Meng, H. X. Zhong, D. Bao, J. M. Yan and X. B. Zhang, *J. Am. Chem. Soc.*, 2016, **138**, 10226–10231.

31 T. J. Schmidt, U. A. Paulus, H. A. Gasteiger and R. J. Behm, *J. Electroanal. Chem.*, 2001, **508**, 41–47.

32 T. M. Arruda, B. Shyam, J. M. Ziegelbauer, S. Mukerjee and D. E. Ramaker, *J. Phys. Chem. C*, 2008, **112**, 18087–18097.

33 G. Horanyi and E. M. Rizmayer, *J. Electroanal. Chem.*, 1977, **83**, 367–373.

34 L. Zhang and S. Mukerjee, *J. Electrochem. Soc.*, 2006, **153**, A1062–A1072.

35 R. F. Lane and A. T. Hubbard, *J. Phys. Chem.*, 1975, **79**, 808–815.

36 N. Job, M. Chatenet, S. Berthon-Fabry, S. Hermans and F. Maillard, *J. Power Sources*, 2013, **240**, 294–305.

37 J. C. Meier, C. Galeano, I. Katsounaros, J. Witte, H. J. Bongard, A. A. Topalov, C. Baldizzone, S. Mezzavilla, F. Schuth and K. J. J. Mayrhofer, *Beilstein J. Nanotechnol.*, 2014, **5**, 44–67.

38 W. T. Hong, M. Risch, K. A. Stoerzinger, A. Grimaud, J. Suntivich and Y. Shao-Horn, *Energy Environ. Sci.*, 2015, **8**, 1404–1427.

39 I. C. Man, H. Y. Su, F. Calle-Vallejo, H. A. Hansen, J. I. Martinez, N. G. Inoglu, J. Kitchin, T. F. Jaramillo, J. K. Norskov and J. Rossmeisl, *ChemCatChem*, 2011, **3**, 1159–1165.

40 M. T. M. Koper, *J. Electroanal. Chem.*, 2011, **660**, 254–260.

41 S. Trasatti, *Electrochim. Acta*, 1984, **29**, 1503–1512.

42 V. Consonni, S. Trasatti, F. Pollak and W. E. Ogrady, *J. Electroanal. Chem.*, 1987, **228**, 393–406.

43 H. A. Hansen, I. C. Man, F. Studt, F. Abild-Pedersen, T. Bligaard and J. Rossmeisl, *Phys. Chem. Chem. Phys.*, 2010, **12**, 283–290.

44 K. S. Exner, J. Anton, T. Jacob and H. Over, *Electrochim. Acta*, 2014, **120**, 460–466.

45 K. S. Exner, J. Anton, T. Jacob and H. Over, *Angew. Chem., Int. Ed.*, 2016, **55**, 7501–7504.

46 R. K. B. Karlsson and A. Cornell, *Chem. Rev.*, 2016, **116**, 2982–3028.

47 K. S. Exner, J. Anton, T. Jacob and H. Over, *Angew. Chem., Int. Ed.*, 2014, **53**, 11032–11035.

48 G. H. Chen, *Sep. Purif. Technol.*, 2004, **38**, 11–41.

49 C. A. Martinez-Huitle and S. Ferro, *Chem. Soc. Rev.*, 2006, **35**, 1324–1340.

50 Y. Kuang, M. J. Kenney, Y. T. Meng, W. H. Hung, Y. J. Liu, J. E. Huang, R. Prasanna, P. S. Li, Y. P. Li, L. Wang, M. C. Lin, M. D. McGehee, X. M. Sun and H. J. Dai, *Proc. Natl. Acad. Sci. U. S. A.*, 2019, **116**, 6624–6629.

51 I. Katsounaros, J. C. Meier and K. J. J. Mayrhofer, *Electrochim. Acta*, 2013, **110**, 790–795.
52 D. Jain, K. Mamtani, V. Gustin, S. Gunduz, G. Celik, I. Waluyo, A. Hunt, A. C. Co and U. S. Ozkan, *ChemElectroChem*, 2018, **5**, 1966–1975.
53 D. Ayed, E. Laubender, M. Souiri, O. Yurchenko, H. Marmouch, G. Urban and A. Othmane, *J. Electrochem. Soc.*, 2017, **164**, B767–B775.
54 C. M. Chung, W. Lee, S. W. Hong and K. Cho, *J. Electrochem. Soc.*, 2019, **166**, H628–H634.
55 M. A. Rahman, X. J. Wang and C. E. Wen, *J. Electrochem. Soc.*, 2013, **160**, A1759–A1771.
56 S. S. Shinde, C. H. Lee, A. Sami, D. H. Kim, S. U. Lee and J. H. Lee, *ACS Nano*, 2017, **11**, 347–357.
57 K. Kishor, S. Saha, M. K. Gupta, A. Bajpai, M. Chatterjee, S. Sivakumar and R. G. S. Pala, *ChemElectroChem*, 2015, **2**, 1839–1846.
58 K. Mamtani, D. Jain, A. C. Co and U. S. Ozkan, *Catal. Lett.*, 2017, **147**, 2903–2909.
59 A. Capelo, M. A. Esteves, A. I. de Sa, R. A. Silva, L. Cangueiro, A. Almeida, R. Vilar and C. M. Rangel, *Int. J. Hydrogen Energy*, 2016, **41**, 12962–12975.
60 J. M. Ziegelbauer, D. Gatewood, A. F. Gulla, M. J. F. Guinel, F. Ernst, D. E. Ramaker and S. Mukerjee, *J. Phys. Chem. C*, 2009, **113**, 6955–6968.
61 J. M. Ziegelbauer, V. S. Murthi, C. O'Laoire, A. F. Guila and S. Mukerjee, *Electrochim. Acta*, 2008, **53**, 5587–5596.
62 D. von Deak, D. Singh, J. C. King and U. S. Ozkan, *Appl. Catal., B*, 2012, **113**, 126–133.
63 D. von Deak, D. Singh, E. J. Biddinger, J. C. King, B. Bayram, J. T. Miller and U. S. Ozkan, *J. Catal.*, 2012, **285**, 145–151.
64 A. Schumpe, I. Adler and W. D. Deckwer, *Biotechnol. Bioeng.*, 1978, **20**, 145–150.
65 N. A. Anastasijevic, Z. M. Dimitrijevic and R. R. Adzic, *Electrochim. Acta*, 1986, **31**, 1125–1130.
66 N. M. Markovic, H. A. Gasteiger, B. N. Grgur and P. N. Ross, *J. Electroanal. Chem.*, 1999, **467**, 157–163.
67 A. F. Gulla, L. Gancs, R. J. Allen and S. Mukerjee, *Appl. Catal., A*, 2007, **326**, 227–235.
68 C. Jin, W. Xia, T. C. Nagaiah, J. S. Guo, X. X. Chen, N. Li, M. Bron, W. Schuhmann and M. Muhler, *J. Mater. Chem.*, 2010, **20**, 736–742.
69 C. Jin, T. C. Nagaiah, W. Xia, M. Bron, W. Schuhmann and M. Muhler, *ChemSusChem*, 2011, **4**, 927–930.
70 X. Y. Wu, X. P. Han, X. Y. Ma, W. Zhang, Y. D. Deng, C. Zhong and W. B. Hu, *ACS Appl. Mater. Interfaces*, 2017, **9**, 12574–12583.
71 Y. P. Deng, Y. Jiang, D. Luo, R. L. Liang, S. B. Cheng, Z. Y. Bai, Y. S. Liu, W. Lei, L. Yang, J. Zhu and Z. W. Chen, *ACS Energy Lett.*, 2017, **2**, 2706–2712.
72 C. C. L. McCrory, S. H. Jung, J. C. Peters and T. F. Jaramillo, *J. Am. Chem. Soc.*, 2013, **135**, 16977–16987.
73 J. G. Vos and M. T. M. Koper, *J. Electroanal. Chem.*, 2018, **819**, 260–268.
74 T. Reier, M. Oezaslan and P. Strasser, *ACS Catal.*, 2012, **2**, 1765–1772.
75 H. N. Nong, H. S. Oh, T. Reier, E. Willinger, M. G. Willinger, V. Petkov, D. Teschner and P. Strasser, *Angew. Chem., Int. Ed.*, 2015, **54**, 2975–2979.
76 H. S. Oh, H. N. Nong, T. Reier, M. Gliech and P. Strasser, *Chem. Sci.*, 2015, **6**, 3321–3328.
77 T. Reier, D. Teschner, T. Lunkenbein, A. Bergmann, S. Selve, R. Kraehnert, R. Schlogl and P. Strasser, *J. Electrochem. Soc.*, 2014, **161**, F876–F882.
78 B. M. Hunter, H. B. Gray and A. M. Muller, *Chem. Rev.*, 2016, **116**, 14120–14136.
79 M. M. Najafpour, G. Renger, M. Holynska, A. N. Moghaddam, E. M. Aro, R. Carpentier, H. Nishihara, J. J. Eaton-Rye, J. R. Shen and S. I. Allakhverdiev, *Chem. Rev.*, 2016, **116**, 2886–2936.
80 T. Takashima, K. Hashimoto and R. Nakamura, *J. Am. Chem. Soc.*, 2012, **134**, 1519–1527.
81 J. E. Bennett, *Int. J. Hydrogen Energy*, 1980, **5**, 401–408.
82 B. J. Trzesniewski, O. Diaz-Morales, D. A. Vermaas, A. Longo, W. Bras, M. T. M. Koper and W. A. Smith, *J. Am. Chem. Soc.*, 2015, **137**, 15112–15121.
83 K. Fan, H. Chen, Y. F. Ji, H. Huang, P. M. Claesson, Q. Daniel, B. Philippe, H. Rensmo, F. S. Li, Y. Luo and L. C. Sun, *Nat. Commun.*, 2016, **7**, 11981.
84 X. Yang, C. J. Wang, C. C. Hou, W. F. Fu and Y. Chen, *ACS Sustainable Chem. Eng.*, 2018, **6**, 2893–2897.
85 M. S. Burke, M. G. Kast, L. Trotochaud, A. M. Smith and S. W. Boettcher, *J. Am. Chem. Soc.*, 2015, **137**, 3638–3648.
86 R. Pokhrel, M. K. Goetz, S. E. Shaner, X. X. Wu and S. S. Stahl, *J. Am. Chem. Soc.*, 2015, **137**, 8384–8387.
87 M. Huynh, D. K. Bediako and D. G. Nocera, *J. Am. Chem. Soc.*, 2014, **136**, 6002–6010.
88 M. Morita, C. Iwakura and H. Tamura, *Electrochim. Acta*, 1977, **22**, 325–328.
89 M. Nakayama, T. Kanaya, J. W. Lee and B. N. Popov, *J. Power Sources*, 2008, **179**, 361–366.
90 I. Zaharieva, P. Chernev, M. Risch, K. Klingan, M. Kohlhoff, A. Fischer and H. Dau, *Energy Environ. Sci.*, 2012, **5**, 7081–7089.
91 J. E. Post, *Proc. Natl. Acad. Sci. U. S. A.*, 1999, **96**, 3447–3454.
92 A. Biswal, B. C. Tripathy, K. Sanjay, T. Subbaiah and M. Minakshi, *RSC Adv.*, 2015, **5**, 58255–58283.
93 M. Nakayama, M. Fukuda, S. Konishi and T. Tonosaki, *J. Mater. Res.*, 2006, **21**, 3152–3160.
94 N. Y. Labrador, E. L. Songcuan, C. De Silva, H. Chen, S. J. Kurdziel, R. K. Ramachandran, C. Detavernier and D. V. Esposito, *ACS Catal.*, 2018, **8**, 1767–1778.
95 A. T. Garcia-Esparza, T. Shinagawa, S. Ould-Chikh, M. Qureshi, X. Y. Peng, N. N. Wei, D. H. Anjum, A. Clo, T. C. Weng, D. Nordlund, D. Sokaras, J. Kubota, K. Domen and K. Takanabe, *Angew. Chem., Int. Ed.*, 2017, **56**, 5780–5784.
96 K. Fujimura, K. Izumiya, A. Kawashima, E. Akiyama, H. Habazaki, N. Kumagai and K. Hashimoto, *J. Appl. Electrochem.*, 1999, **29**, 765–771.
97 N. A. A. Ghany, N. Kumagai, S. Meguro, K. Asami and K. Hashimoto, *Electrochim. Acta*, 2002, **48**, 21–28.
98 Z. Kato, J. Bhattarai, N. Kumagai, K. Izumiya and K. Hashimoto, *Appl. Surf. Sci.*, 2011, **257**, 8230–8236.

99 R. Balaji, S. K. Balasingam, J. Lakshmi, N. Senthil, S. Vasudevan, G. Sozhan, A. K. Shukla and S. Ravichandran, *Electrochem. Commun.*, 2009, **11**, 1700–1702.

100 M. Sakashita and N. Sato, *Corrosion*, 1979, **35**, 351–355.

101 M. Sakashita and N. Sato, *Corros. Sci.*, 1977, **17**, 473–486.

102 I. Roger, M. A. Shipman and M. D. Symes, *Nat. Rev. Chem.*, 2017, **1**, 0003.

103 Z. W. Seh, J. Kibsgaard, C. F. Dickens, I. B. Chorkendorff, J. K. Norskov and T. F. Jaramillo, *Science*, 2017, **355**, eaad4998.

104 Q. Ding, B. Song, P. Xu and S. Jin, *Chem*, 2016, **1**, 699–726.

105 E. Fabbri, M. Nachtegaal, T. Binninger, X. Cheng, B. J. Kim, J. Durst, F. Bozza, T. Graule, R. Schaublin, L. Wiles, M. Pertoso, N. Danilovic, K. E. Ayers and T. J. Schmidt, *Nat. Mater.*, 2017, **16**, 925–931.

106 I. Ledezma-Yanez, W. D. Z. Wallace, P. Sebastian-Pascual, V. Climent, J. M. Feliu and M. T. M. Koper, *Nat. Energy*, 2017, **2**, 17031.

107 H. J. Song, H. Yoon, B. Ju, D. Y. Lee and D. W. Kim, *ACS Catal.*, 2020, **10**, 702–709.

108 F. Z. Song, W. Li, J. Q. Yang, G. Q. Han, P. L. Liao and Y. J. Sun, *Nat. Commun.*, 2018, **9**, 4531.

109 Y. Wang, Y. Sun, F. Yan, C. L. Zhu, P. Gao, X. T. Zhang and Y. J. Chen, *J. Mater. Chem. A*, 2018, **6**, 8479–8487.

110 C. L. Zhu, Z. X. Yin, W. H. Lai, Y. Sun, L. N. Liu, X. T. Zhang, Y. J. Chen and S. L. Chou, *Adv. Energy Mater.*, 2018, **8**, 1802327.

111 L. Yu, Q. Zhu, S. W. Song, B. McElhenny, D. Z. Wang, C. Z. Wu, Z. J. Qin, J. M. Bao, Y. Yu, S. Chen and Z. F. Ren, *Nat. Commun.*, 2019, **10**, 5106.

112 F. F. Cheng, X. L. Feng, X. Chen, W. G. Lin, J. F. Rong and W. S. Yang, *Electrochim. Acta*, 2017, **251**, 336–343.

113 Y. Q. Zhao, B. Jin, Y. Zheng, H. Y. Jin, Y. Jiao and S. Z. Qiao, *Adv. Energy Mater.*, 2018, **8**, 1801926.

114 Y. Q. Zhao, B. Jin, A. Vasileff, Y. Jiao and S. Z. Qiao, *J. Mater. Chem. A*, 2019, **7**, 8117–8121.

115 H. Li, Q. Tang, B. He and P. Yang, *J. Mater. Chem. A*, 2016, **4**, 6513–6520.

116 S. H. Hsu, J. W. Miao, L. P. Zhang, J. J. Gao, H. M. Wang, H. B. Tao, S. F. Hung, A. Vasileff, S. Z. Qiao and B. Liu, *Adv. Mater.*, 2018, **30**, 1707261.

117 I. C. Blake, *J. Electrochem. Soc.*, 1952, **99**, C202–C203.

118 L. E. Pucher, *J. Electrochem. Soc.*, 1952, **99**, C203–C204.

119 J. R. Coleman, *J. Appl. Electrochem.*, 1971, **1**, 65–71.

120 K. V. Prasad, N. Venkatakrishnan and P. B. Mathur, *J. Power Sources*, 1977, **1**, 371–375.

121 R. Renuka, *J. Appl. Electrochem.*, 1997, **27**, 1394–1397.

122 Q. F. Liu, Z. Yan, E. D. Wang, S. L. Wang and G. Q. Sun, *Int. J. Hydrogen Energy*, 2017, **42**, 23045–23053.

123 P. K. Shen, A. C. C. Tseung and C. Kuo, *J. Power Sources*, 1994, **47**, 119–127.

124 B. M. L. Rao, W. H. Hoge, J. Zakrzewski, S. Shah and W. Halliop, *Proceedings of the 6th International Symposium on Unmanned Untethered Submersible Technology (IEEE)*, July, 1989.

125 H. Y. Zhao, P. Bian and D. Y. Ju, *J. Environ. Sci.*, 2009, **21**(Suppl 1), S88–S91.

126 W. S. D. Wilcock and P. C. Kauffman, *J. Power Sources*, 1997, **66**, 71–75.

127 D. T. Welna, D. A. Stone and H. R. Allcock, *Chem. Mater.*, 2006, **18**, 4486–4492.

128 R. E. Davis and J. T. Sherman, *J. Atoms. Oceanic Technol.*, 2017, **34**, 1175–1182.

129 J. K. Kim, F. Mueller, H. Kim, D. Bresser, J. S. Park, D. H. Lim, G. T. Kim, S. Passerini and Y. Kim, *NPG Asia Mater.*, 2014, **6**, e144.

130 J. Han, S. M. Hwang, W. Go, S. T. Senthilkumar, D. Jeon and Y. Kim, *J. Power Sources*, 2018, **374**, 24–30.

131 Y. Kim, S. M. Hwang and H. Yu, *J. Mater. Chem. A*, 2018, **6**, 3046–3054.

132 Y. Kim, J. K. Kim, C. Vaalma, G. H. Bae, G. T. Kim and S. Passerini, *Carbon*, 2018, **129**, 564–571.

133 N. D. K. Tu, S. O. Park, J. Park, Y. Kim, S. K. Kwak and S. J. Kang, *ACS Appl. Energy Mater.*, 2020, **3**, 1602–1608.

134 M. Abirami, S. M. Hwang, J. Yang, S. T. Senthilkumar, J. Kim, W. S. Go, B. Senthilkumar, H. K. Song and Y. Kim, *ACS Appl. Mater. Interfaces*, 2016, **8**, 32778–32787.

135 J. J. Duan, S. Chen, A. Vasileff and S. Z. Qiao, *ACS Nano*, 2016, **10**, 8738–8745.

136 C. Tang, B. Wang, H. F. Wang and Q. Zhang, *Adv. Mater.*, 2017, **29**, 1703185.

137 I. Yamada, H. Fujii, A. Takamatsu, H. Ikeno, K. Wada, H. Tsukasaki, S. Kawaguchi, S. Mori and S. Yagi, *Adv. Mater.*, 2017, **29**, 1603004.

138 R. Hahn, J. Mainert, F. Glaw and K. D. Lang, *J. Power Sources*, 2015, **288**, 26–35.

139 S. Al Bacha, I. Aubert, O. Devos, M. Zakhour, M. Nakhl and J. L. Bobet, *Int. J. Hydrogen Energy*, 2020, **45**, 15805–15813.

140 T. H. Wu, Y. M. Zhang, Z. D. Althouse and N. Liu, *Mater. Today. Nano*, 2019, **6**, 100032.

141 Y. Kim, H. Kim, S. Park and I. Seo, *Electrochim. Acta*, 2016, **191**, 1–7.

142 Y. Kim, G. T. Kim, S. Jeong, X. W. Dou, C. X. Geng and S. Passerini, *Energy Storage Mater.*, 2019, **16**, 56–64.